Measurement of the Time-Dependent *CP* Asymmetry of Partially Reconstructed $B^0 \to D^{*+}D^{*-}$ Decays

J. P. Lees, V. Poireau, and V. Tisserand
*Laboratoire d'Annecy-le-Vieux de Physique des Particules (LAPP),
Université de Savoie, CNRS/IN2P3, F-74941 Annecy-Le-Vieux, France*

J. Garra Tico and E. Grauges
Universitat de Barcelona, Facultat de Fisica, Departament ECM, E-08028 Barcelona, Spain

A. Palano[ab]
INFN Sezione di Bari[a]; Dipartimento di Fisica, Università di Bari[b], I-70126 Bari, Italy

G. Eigen and B. Stugu
University of Bergen, Institute of Physics, N-5007 Bergen, Norway

D. N. Brown, L. T. Kerth, Yu. G. Kolomensky, and G. Lynch
Lawrence Berkeley National Laboratory and University of California, Berkeley, California 94720, USA

H. Koch and T. Schroeder
Ruhr Universität Bochum, Institut für Experimentalphysik 1, D-44780 Bochum, Germany

D. J. Asgeirsson, C. Hearty, T. S. Mattison, J. A. McKenna, and R. Y. So
University of British Columbia, Vancouver, British Columbia, Canada V6T 1Z1

A. Khan
Brunel University, Uxbridge, Middlesex UB8 3PH, United Kingdom

V. E. Blinov, A. R. Buzykaev, V. P. Druzhinin, V. B. Golubev, E. A. Kravchenko, A. P. Onuchin,
S. I. Serednyakov, Yu. I. Skovpen, E. P. Solodov, K. Yu. Todyshev, and A. N. Yushkov
Budker Institute of Nuclear Physics, Novosibirsk 630090, Russia

M. Bondioli, D. Kirkby, A. J. Lankford, and M. Mandelkern
University of California at Irvine, Irvine, California 92697, USA

H. Atmacan, J. W. Gary, F. Liu, O. Long, and G. M. Vitug
University of California at Riverside, Riverside, California 92521, USA

C. Campagnari, T. M. Hong, D. Kovalskyi, J. D. Richman, and C. A. West
University of California at Santa Barbara, Santa Barbara, California 93106, USA

A. M. Eisner, J. Kroseberg, W. S. Lockman, A. J. Martinez, B. A. Schumm, and A. Seiden
University of California at Santa Cruz, Institute for Particle Physics, Santa Cruz, California 95064, USA

D. S. Chao, C. H. Cheng, B. Echenard, K. T. Flood, D. G. Hitlin, P. Ongmongkolkul, F. C. Porter, and A. Y. Rakitin
California Institute of Technology, Pasadena, California 91125, USA

R. Andreassen, Z. Huard, B. T. Meadows, M. D. Sokoloff, and L. Sun
University of Cincinnati, Cincinnati, Ohio 45221, USA

P. C. Bloom, W. T. Ford, A. Gaz, U. Nauenberg, J. G. Smith, and S. R. Wagner
University of Colorado, Boulder, Colorado 80309, USA

R. Ayad* and W. H. Toki
Colorado State University, Fort Collins, Colorado 80523, USA

B. Spaan
Technische Universität Dortmund, Fakultät Physik, D-44221 Dortmund, Germany

K. R. Schubert and R. Schwierz
Technische Universität Dresden, Institut für Kern- und Teilchenphysik, D-01062 Dresden, Germany

D. Bernard and M. Verderi
Laboratoire Leprince-Ringuet, Ecole Polytechnique, CNRS/IN2P3, F-91128 Palaiseau, France

P. J. Clark and S. Playfer
University of Edinburgh, Edinburgh EH9 3JZ, United Kingdom

D. Bettoni[a], C. Bozzi[a], R. Calabrese[ab], G. Cibinetto[ab], E. Fioravanti[ab],
I. Garzia[ab], E. Luppi[ab], M. Munerato[ab], L. Piemontese[a], and V. Santoro[a]
INFN Sezione di Ferrara[a]; Dipartimento di Fisica, Università di Ferrara[b], I-44100 Ferrara, Italy

R. Baldini-Ferroli, A. Calcaterra, R. de Sangro, G. Finocchiaro,
P. Patteri, I. M. Peruzzi,[†] M. Piccolo, M. Rama, and A. Zallo
INFN Laboratori Nazionali di Frascati, I-00044 Frascati, Italy

R. Contri[ab], E. Guido[ab], M. Lo Vetere[ab], M. R. Monge[ab], S. Passaggio[a], C. Patrignani[ab], and E. Robutti[a]
INFN Sezione di Genova[a]; Dipartimento di Fisica, Università di Genova[b], I-16146 Genova, Italy

B. Bhuyan and V. Prasad
Indian Institute of Technology Guwahati, Guwahati, Assam, 781 039, India

C. L. Lee and M. Morii
Harvard University, Cambridge, Massachusetts 02138, USA

A. J. Edwards
Harvey Mudd College, Claremont, California 91711, USA

A. Adametz and U. Uwer
Universität Heidelberg, Physikalisches Institut, Philosophenweg 12, D-69120 Heidelberg, Germany

H. M. Lacker and T. Lueck
Humboldt-Universität zu Berlin, Institut für Physik, Newtonstr. 15, D-12489 Berlin, Germany

P. D. Dauncey
Imperial College London, London, SW7 2AZ, United Kingdom

U. Mallik
University of Iowa, Iowa City, Iowa 52242, USA

C. Chen, J. Cochran, W. T. Meyer, S. Prell, and A. E. Rubin
Iowa State University, Ames, Iowa 50011-3160, USA

A. V. Gritsan and Z. J. Guo
Johns Hopkins University, Baltimore, Maryland 21218, USA

N. Arnaud, M. Davier, D. Derkach, G. Grosdidier, F. Le Diberder, A. M. Lutz,
B. Malaescu, P. Roudeau, M. H. Schune, A. Stocchi, and G. Wormser
*Laboratoire de l'Accélérateur Linéaire, IN2P3/CNRS et Université Paris-Sud 11,
Centre Scientifique d'Orsay, B. P. 34, F-91898 Orsay Cedex, France*

D. J. Lange and D. M. Wright
Lawrence Livermore National Laboratory, Livermore, California 94550, USA

C. A. Chavez, J. P. Coleman, J. R. Fry, E. Gabathuler, D. E. Hutchcroft, D. J. Payne, and C. Touramanis
University of Liverpool, Liverpool L69 7ZE, United Kingdom

A. J. Bevan, F. Di Lodovico, R. Sacco, and M. Sigamani

Queen Mary, University of London, London, E1 4NS, United Kingdom

G. Cowan

University of London, Royal Holloway and Bedford New College, Egham, Surrey TW20 0EX, United Kingdom

D. N. Brown and C. L. Davis

University of Louisville, Louisville, Kentucky 40292, USA

A. G. Denig, M. Fritsch, W. Gradl, K. Griessinger, A. Hafner, and E. Prencipe

Johannes Gutenberg-Universität Mainz, Institut für Kernphysik, D-55099 Mainz, Germany

R. J. Barlow,[‡] G. Jackson, and G. D. Lafferty

University of Manchester, Manchester M13 9PL, United Kingdom

E. Behn, R. Cenci, B. Hamilton, A. Jawahery, and D. A. Roberts

University of Maryland, College Park, Maryland 20742, USA

C. Dallapiccola

University of Massachusetts, Amherst, Massachusetts 01003, USA

R. Cowan, D. Dujmic, and G. Sciolla

Massachusetts Institute of Technology, Laboratory for Nuclear Science, Cambridge, Massachusetts 02139, USA

R. Cheaib, D. Lindemann, P. M. Patel,[§] and S. H. Robertson

McGill University, Montréal, Québec, Canada H3A 2T8

P. Biassoni[ab], N. Neri[a], F. Palombo[ab], and S. Stracka[ab]

INFN Sezione di Milano[a]; Dipartimento di Fisica, Università di Milano[b], I-20133 Milano, Italy

L. Cremaldi, R. Godang,[¶] R. Kroeger, P. Sonnek, and D. J. Summers

University of Mississippi, University, Mississippi 38677, USA

X. Nguyen, M. Simard, and P. Taras

Université de Montréal, Physique des Particules, Montréal, Québec, Canada H3C 3J7

G. De Nardo[ab], D. Monorchio[ab], G. Onorato[ab], and C. Sciacca[ab]

INFN Sezione di Napoli[a]; Dipartimento di Scienze Fisiche,
Università di Napoli Federico II[b], I-80126 Napoli, Italy

M. Martinelli and G. Raven

NIKHEF, National Institute for Nuclear Physics and High Energy Physics, NL-1009 DB Amsterdam, The Netherlands

C. P. Jessop, J. M. LoSecco, and W. F. Wang

University of Notre Dame, Notre Dame, Indiana 46556, USA

K. Honscheid and R. Kass

Ohio State University, Columbus, Ohio 43210, USA

J. Brau, R. Frey, N. B. Sinev, D. Strom, and E. Torrence

University of Oregon, Eugene, Oregon 97403, USA

E. Feltresi[ab], N. Gagliardi[ab], M. Margoni[ab], M. Morandin[a],
M. Posocco[a], M. Rotondo[a], G. Simi[a], F. Simonetto[ab], and R. Stroili[ab]

INFN Sezione di Padova[a]; Dipartimento di Fisica, Università di Padova[b], I-35131 Padova, Italy

S. Akar, E. Ben-Haim, M. Bomben, G. R. Bonneaud, H. Briand, G. Calderini,
J. Chauveau, O. Hamon, Ph. Leruste, G. Marchiori, J. Ocariz, and S. Sitt

Laboratoire de Physique Nucléaire et de Hautes Energies,
IN2P3/CNRS, Université Pierre et Marie Curie-Paris6,
Université Denis Diderot-Paris7, F-75252 Paris, France

M. Biasini[ab], E. Manoni[ab], S. Pacetti[ab], and A. Rossi[ab]
INFN Sezione di Perugia[a]; Dipartimento di Fisica, Università di Perugia[b], I-06100 Perugia, Italy

C. Angelini[ab], G. Batignani[ab], S. Bettarini[ab], M. Carpinelli[ab],[**] G. Casarosa[ab], A. Cervelli[ab], F. Forti[ab],
M. A. Giorgi[ab], A. Lusiani[ac], B. Oberhof[ab], E. Paoloni[ab], A. Perez[a], G. Rizzo[ab], and J. J. Walsh[a]
INFN Sezione di Pisa[a]; Dipartimento di Fisica, Università di Pisa[b]; Scuola Normale Superiore di Pisa[c], I-56127 Pisa, Italy

D. Lopes Pegna, J. Olsen, A. J. S. Smith, and A. V. Telnov
Princeton University, Princeton, New Jersey 08544, USA

F. Anulli[a], R. Faccini[ab], F. Ferrarotto[a], F. Ferroni[ab], M. Gaspero[ab], L. Li Gioi[a], M. A. Mazzoni[a], and G. Piredda[a]
INFN Sezione di Roma[a]; Dipartimento di Fisica,
Università di Roma La Sapienza[b], I-00185 Roma, Italy

C. Bünger, O. Grünberg, T. Hartmann, T. Leddig, H. Schröder,[§] C. Voss, and R. Waldi
Universität Rostock, D-18051 Rostock, Germany

T. Adye, E. O. Olaiya, and F. F. Wilson
Rutherford Appleton Laboratory, Chilton, Didcot, Oxon, OX11 0QX, United Kingdom

S. Emery, G. Hamel de Monchenault, G. Vasseur, and Ch. Yèche
CEA, Irfu, SPP, Centre de Saclay, F-91191 Gif-sur-Yvette, France

D. Aston, D. J. Bard, R. Bartoldus, J. F. Benitez, C. Cartaro, M. R. Convery, J. Dorfan, G. P. Dubois-Felsmann,
W. Dunwoodie, M. Ebert, R. C. Field, M. Franco Sevilla, B. G. Fulsom, A. M. Gabareen, M. T. Graham,
P. Grenier, C. Hast, W. R. Innes, M. H. Kelsey, P. Kim, M. L. Kocian, D. W. G. S. Leith, P. Lewis, B. Lindquist,
S. Luitz, V. Luth, H. L. Lynch, D. B. MacFarlane, D. R. Muller, H. Neal, S. Nelson, M. Perl, T. Pulliam,
B. N. Ratcliff, A. Roodman, A. A. Salnikov, R. H. Schindler, A. Snyder, D. Su, M. K. Sullivan, J. Va'vra,
A. P. Wagner, W. J. Wisniewski, M. Wittgen, D. H. Wright, H. W. Wulsin, C. C. Young, and V. Ziegler
SLAC National Accelerator Laboratory, Stanford, California 94309 USA

W. Park, M. V. Purohit, R. M. White, and J. R. Wilson
University of South Carolina, Columbia, South Carolina 29208, USA

A. Randle-Conde and S. J. Sekula
Southern Methodist University, Dallas, Texas 75275, USA

M. Bellis, P. R. Burchat, T. S. Miyashita, and E. M. T. Puccio
Stanford University, Stanford, California 94305-4060, USA

M. S. Alam and J. A. Ernst
State University of New York, Albany, New York 12222, USA

R. Gorodeisky, N. Guttman, D. R. Peimer, and A. Soffer
Tel Aviv University, School of Physics and Astronomy, Tel Aviv, 69978, Israel

P. Lund and S. M. Spanier
University of Tennessee, Knoxville, Tennessee 37996, USA

J. L. Ritchie, A. M. Ruland, R. F. Schwitters, and B. C. Wray
University of Texas at Austin, Austin, Texas 78712, USA

J. M. Izen and X. C. Lou
University of Texas at Dallas, Richardson, Texas 75083, USA

F. Bianchi[ab], D. Gamba[ab], and S. Zambito[ab]

INFN Sezione di Torino[a]; Dipartimento di Fisica Sperimentale, Università di Torino[b], I-10125 Torino, Italy

L. Lanceri[ab] and L. Vitale[ab]

INFN Sezione di Trieste[a]; Dipartimento di Fisica, Università di Trieste[b], I-34127 Trieste, Italy

F. Martinez-Vidal and A. Oyanguren

IFIC, Universitat de Valencia-CSIC, E-46071 Valencia, Spain

H. Ahmed, J. Albert, Sw. Banerjee, F. U. Bernlochner, H. H. F. Choi, G. J. King,
R. Kowalewski, M. J. Lewczuk, I. M. Nugent, J. M. Roney, R. J. Sobie, and N. Tasneem

University of Victoria, Victoria, British Columbia, Canada V8W 3P6

T. J. Gershon, P. F. Harrison, and T. E. Latham

Department of Physics, University of Warwick, Coventry CV4 7AL, United Kingdom

H. R. Band, S. Dasu, Y. Pan, R. Prepost, and S. L. Wu

University of Wisconsin, Madison, Wisconsin 53706, USA

(Dated: 26 July, 2012)

We present a new measurement of the time-dependent CP asymmetry of $B^0 \to D^{*+}D^{*-}$ decays using (471 ± 5) million $B\bar{B}$ pairs collected with the *BABAR* detector at the PEP-II B Factory at the SLAC National Accelerator Laboratory. Using the technique of partial reconstruction, we measure the time-dependent CP asymmetry parameters $S = -0.34 \pm 0.12 \pm 0.05$ and $C = +0.15 \pm 0.09 \pm 0.04$. Using the value for the CP-odd fraction $R_\perp = 0.158 \pm 0.028 \pm 0.006$, previously measured by *BABAR* with fully reconstructed $B^0 \to D^{*+}D^{*-}$ events, we extract the CP-even components $S_+ = -0.49 \pm 0.18 \pm 0.07 \pm 0.04$ and $C_+ = +0.15 \pm 0.09 \pm 0.04$. In each case, the first uncertainty is statistical and the second is systematic; the third uncertainty on S_+ is the contribution from the uncertainty on $R_\perp$. The measured value of the CP-even component S_+ is consistent with the value of $\sin 2\beta$ measured in $b \to (c\bar{c})s$ transitions, and with the Standard Model expectation of small penguin contributions.

PACS numbers: 13.25.Hw, 12.15.Hh, 11.30.Er

I. INTRODUCTION

In the Standard Model (SM), CP violation arises from an irreducible complex phase in the 3×3 quark mixing matrix V known as the Cabibbo-Kobayashi-Maskawa (CKM) matrix [1, 2]. Unitarity of the CKM matrix requires that the relation $V_{ud}V_{ub}^* + V_{cd}V_{cb}^* + V_{td}V_{tb}^* = 0$, which defines the unitarity triangle, be satisfied. The aim of the B Factories is to test the unitarity of the CKM matrix by the precise measurement of the angles and sides of the above triangle, whose nonvanishing area indicates violation of CP symmetry.

Both the *BABAR* and Belle collaborations have measured the CP parameter $\sin 2\beta$, where the angle β is de-
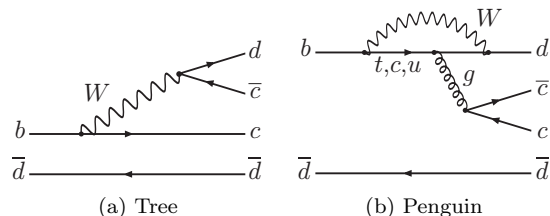
———

*Now at the University of Tabuk, Tabuk 71491, Saudi Arabia

†Also with Università di Perugia, Dipartimento di Fisica, Perugia, Italy

‡Now at the University of Huddersfield, Huddersfield HD1 3DH, UK

§Deceased

¶Now at University of South Alabama, Mobile, Alabama 36688, USA

**Also with Università di Sassari, Sassari, Italy

FIG. 1: Leading and sub-leading order Feynman graphs for the $\bar{B}^0 \to D^{(*)+}D^{(*)-}$ decays.

fined as $\beta \equiv \arg[-V_{cd}V_{cb}^*/V_{td}V_{tb}^*]$. The most accurate measurements of $\sin 2\beta$ [3–5] use the $b \to (c\bar{c})s$ transition, in which B^0's decay to charmonium final states. Measurement of $b \to c\bar{c}d$ transitions such as $B^0 \to D^{(*)+}D^{(*)-}$ should yield the same value of $\sin 2\beta$ to the extent that the contributions from penguin processes may be neglected.

The leading and sub-leading order Feynman diagrams contributing to $B^0 \to D^{(*)+}D^{(*)-}$ decays are shown in Fig. 1. The effect of neglecting the penguin amplitude has been estimated in models based on factorization and heavy quark symmetry, and the corrections are found to be a few percent [6, 7]. Loops involving non-SM particles (for example, charged Higgs or SUSY particles) could increase the contribution from penguin diagrams and in-

troduce additional phases.

In $\Upsilon(4S) \rightarrow B^0\overline{B}^0$ events the time-dependent decay rate for $B^0 \rightarrow D^{*+}D^{*-}$ is given by

$$
\begin{aligned}
P_\eta^{S_{\text{tag}}}(\Delta t) = & \frac{e^{-|\Delta t|/\tau_b}}{4\tau_b} \cdot [1 + S_{\text{tag}} S_\eta \sin(\Delta m_d \Delta t) \\
& + S_{\text{tag}} C \cos(\Delta m_d \Delta t)],
\end{aligned} \tag{1}
$$

where τ_b is the B^0 lifetime averaged over the two mass eigenstates, Δm_d is the $B^0\overline{B}^0$ mixing frequency, and Δt is the time interval between the $B^0 \rightarrow D^{*+}D^{*-}$ decay (B_{rec}) and the decay of the other B (B_{tag}) in the event. The parameter $S_{\text{tag}} = +1 \ (-1)$ in Eq. (1) indicates the flavor of the B_{tag} as a $B^0 \ (\overline{B}^0)$, while $\eta = \pm 1$ indicates the CP eigenvalue of the $B^0 \rightarrow D^{*+}D^{*-}$ final state. The parameters C and S_η are given by

$$
C = \frac{1 - |\lambda|^2}{1 + |\lambda|^2}; \quad S_\eta = -\eta \frac{2\Im m(\lambda)}{1 + |\lambda|^2}; \quad \lambda = \frac{q}{p} \frac{\overline{A}}{A}, \tag{2}
$$

where $A \ (\overline{A})$ is the matrix element of the $B^0 \ (\overline{B}^0)$ decay and p and q are the coefficients appearing in the expression of the physical mass eigenstates B_L, B_H in terms of the flavour eigenstates B, $\overline{B}$:

$$
\begin{aligned}
|B_L\rangle &= p|B\rangle + q|\overline{B}\rangle \\
|B_H\rangle &= p|B\rangle - q|\overline{B}\rangle.
\end{aligned}
$$

Since the $B^0 \rightarrow D^{*+}D^{*-}$ is the decay of a scalar to two vector mesons, the final state is a mixture of CP eigenstates. The CP-odd and CP-even fractions have been previously measured from the angular analysis of completely reconstructed events [8, 9].

A large deviation of the measured parameter S_η in Eq. 2 from the value of $\sin 2\beta$ measured in $b \rightarrow (c\overline{c})s$ transitions or a non-zero value of direct CP violation [10–12] would be strong evidence of new physics.

Both the BABAR [8] and Belle [9] collaborations have studied the CP asymmetries of $B^0 \rightarrow D^{*+}D^{*-}$ decays using fully reconstructed events. In this article we report a new measurement based on the technique of partial reconstruction, which allows us to gain a factor of $\simeq 5$ in the number of selected signal events with respect to the most recent BABAR full reconstruction analysis in [8]. This result is complementary to the latter measurement, because the statistics used are largely independent of each other.

II. THE BABAR DETECTOR AND DATASET

The data sample used in this analysis has been collected with the BABAR detector [13] operating at the PEP-II asymmetric-energy B Factory located at the SLAC National Accelerator Laboratory. We have analyzed the full BABAR data set collected at the the $\Upsilon(4S)$ mass peak, $\sqrt{s} = 10.58$ GeV, corresponding to an integrated luminosity of 429.0 fb^{-1}. In addition, we have used 44.8 fb^{-1}

of data taken off-resonance to evaluate the background from events $e^+e^- \rightarrow q\overline{q}$, where q represents a u, d, s or c quark ("continuum"). To study backgrounds and validate the analysis procedure, we use a GEANT4-based [14] Monte Carlo (MC) simulation in which coherent $B\overline{B}$ production is simulated using the package EvtGen [15].

The asymmetric energies of the PEP-II beams are an ideal environment to study time-dependent CP phenomena in the B^0-$\overline{B}^0$ system. The boost of the $\Upsilon(4S)$ in the laboratory frame by $\beta\gamma = 0.56$ increases the separation between the vertices of the two B meson daughters, allowing their precise measurement.

The BABAR detector is described in detail in Ref. [13]. We give here only a brief description of the main components and their use in this analysis. Tracking is provided by a five-layer silicon vertex detector (SVT) and a drift chamber (DCH). The SVT provides precise position measurements close to the interaction region that are used in vertex reconstruction and low-momentum track reconstruction. The DCH provides excellent momentum measurement of charged particles.

Particle identification (PID) of kaons and pions is obtained from ionization losses in the SVT and DCH and from measurements of photons produced in a ring-imaging Cherenkov light detector (DIRC). A CsI(Tl) crystal-based electromagnetic calorimeter (EMC) enables measurement of photon energies and electron identification. These systems all operate inside a 1.5 T superconducting solenoid, whose iron flux return is instrumented for muon detection, initially with resistive plate chambers and more recently with limited streamer tubes [16].

III. ANALYSIS METHOD

A. Partial Reconstruction

In the partial reconstruction of a $B^0 \rightarrow D^{*+}D^{*-}$ candidate, we reconstruct fully only one of the two $D^{*\pm}$ mesons in the decay chain $D^* \rightarrow D^0\pi$ [17], by identifying D^0 candidates in one of four final states: $K\pi$, $K\pi\pi^0$, $K\pi\pi\pi$, $K_S^0\pi\pi$. The vertexing algorithm fits the two-step decay tree simultaneously, correctly calculating correlations among all candidates. In the first three D^0 decay modes, assumed to represent Cabibbo-favored decays, charged kaon tracks are selected using PID information from the DIRC, SVT and DCH. In the last decay mode, K_S^0 candidates are selected by constraining pairs of oppositely charged tracks to a common vertex.

Since the kinetic energy available in the decay $D^* \rightarrow D^0 \pi$ is small, we combine one reconstructed $D^{*\pm}$ with an oppositely charged low-momentum pion, assumed to originate from the decay of the unreconstructed $D^{*\mp}$, and evaluate the mass m_{rec} of the recoiling D^0 meson by using the momenta of the two particles. For signal events m_{rec} peaks at the nominal D^0 mass [18] with an r.m.s. width of about 3 MeV/c^2, while for background events no such peak is visible. Thus, m_{rec} is the primary variable to

discriminate signal from background. The calculation of $m_{\rm rec}$ proceeds as follows (refer to Fig. 2 for definitions of the various momenta and angles that we use).
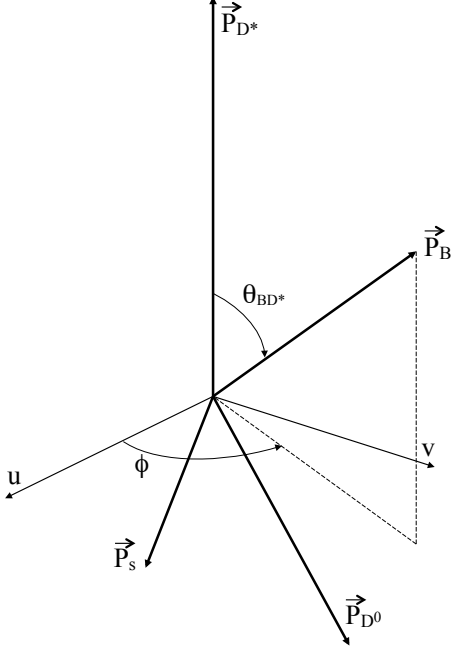

FIG. 2: Momenta and angles in the $\Upsilon(4S)$ center of mass frame used in partial reconstruction. The orthogonal axes u and v are normal to the momentum $\vec{p}_{D^*}$ of the reconstructed D^*, and u lies in the plane defined by the momenta of the D^* and slow pion, $\vec{p}_{D^*}$ and $\vec{p}_s$. The angle ϕ is measured in the $u - v$ plane.

The cosine of the angle between the momenta in the $\Upsilon(4S)$ center of mass (CM) frame of the B and the reconstructed D^* is readily computed:

$$\cos\theta_{BD^*} = \frac{-M_{B^0}^2 + E_{\rm CM}E_{D^*}}{2p_B|\vec{p}_{D^*}|}, \qquad (3)$$

where all particle masses are set to their nominal values [18], E_{D^*} and $\vec{p}_{D^*}$ are the measured energy and momentum of the reconstructed D^* in the $\Upsilon(4S)$ CM frame, $E_{\rm CM}/2$ is the energy of each beam in the CM frame, and $p_B = \sqrt{E_{\rm CM}^2/4 - M_{B^0}^2}$ is the B-meson CM momentum. Events are required to be in the physical region $|\cos\theta_{BD^*}| < 1$.

Given $\cos\theta_{BD^*}$ and the measured momenta of the D^* and oppositely charged low-momentum pion, π_s, the B four-momentum can be calculated up to an unknown azimuthal angle ϕ around $\vec{p}_{D^*}$. For any chosen value of ϕ, conservation laws determine the unreconstructed D^0 four-momentum $q_D(\phi)$, and one can thus compute

the corresponding ϕ-dependent invariant mass $m(\phi) \equiv \sqrt{|q_D(\phi)|^2}$. The value of ϕ is not constrained by kinematics and may be chosen arbitrarily, to the extent that the shape of the resulting $m(\phi)$ distribution may still be described by the type of functions used in our fits. We have chosen the value for which $\cos\phi = 0.62$, which is the median of the corresponding Monte Carlo distribution for signal events obtained using generated momenta, and define the recoiling D^0 mass $m_{\rm rec} \equiv m(\cos\phi{=}0.62)$. We use the same convention to obtain the direction of the unreconstructed D^0 meson.

B. Backgrounds and Event Selection

Backgrounds to the $B^0 \rightarrow D^{*+}D^{*-}$ process include the following:

- Combinatorial $B\bar{B}$ background, defined as decays other than $B^0 \rightarrow D^{*+}D^{*-}$, for which the $m_{\rm rec}$ distribution is approximately flat.

- Peaking $B\bar{B}$ background, defined as decays other than $B^0 \rightarrow D^{*+}D^{*-}$, in which the $m_{\rm rec}$ distribution peaks in the signal region. It will be shown later that the contribution from this background is negligible.

- Background from non-$b\bar{b}$ events.

Combinatorial $B\bar{B}$ background events are reduced by the following requirements: For the $K_S^0\pi\pi$ mode, we require the invariant mass of the pion pair to be within 25 MeV/c^2 of the K_S^0 mass [18]. The corresponding vertex must be separated by more than 3 mm from the beam axis. For the $K\pi\pi^0$ mode, π^0 candidates are formed from pairs of photons detected in the EMC, with energies greater than 40 MeV, for which the invariant mass differs by less than 20 MeV/c^2 from the nominal π^0 mass [18]. The reconstructed D^0 mass must be equal to the nominal one [18] within 2 or 2.5 standard deviations, depending on the D^0 reconstruction mode. The momenta in the $\Upsilon(4S)$ CM frame of the reconstructed D^* and π_s from the missing D^0 must be, respectively, in the range 1.3–2.1 GeV/c and smaller than 0.6 GeV/c. The difference $\Delta M = |M_{D^*} - M_{D^0} - M_\pi|$ must be equal to the nominal [18] value within 1 or 1.5 MeV/c^2, according to the presence or absence of DCH hits in the pion track appearing in the reconstructed decay $D^* \rightarrow D^0\,\pi$. The probability of the vertex fits must be greater than 10^{-2}, for both the D^0 and the D^* reconstruction.

The requirement on the D^0 vertex fit probability introduces a small but measurable bias toward lower values of the B lifetime. Due to partial reconstruction, the tracks used to make the D^0 vertex may originate from the same or different B mesons. In the latter case, since not all tracks are from the same point in space, the χ^2 of the vertex fit tends to be bigger. This effect worsens with increasing distance between the two B decay vertices, causing vertices further apart to be rejected more frequently.

We have verified this on signal Monte Carlo events, for which we have measured a lifetime lower than the generated value. Consequently, for the signal Δt probability distribution functions (PDF's) we use the value of τ_b fitted to signal Monte Carlo.

In events passing this selection we find more than one candidate decay chain in about 25% of the cases, usually differing only in the slow pion π_s, but sometimes in the components of the reconstructed D^*. When this happens, we choose one candidate chain, based respectively on the largest number of DCH hits in the π_s, or according to a χ^2 based on the reconstructed D^0 mass and ΔM quantity above. For signal Monte Carlo, the probability for this candidate chain to be the correct one is 0.95.

The main suppression of continuum background is obtained by requiring that the ratio R_2 of the 2nd to the 0th Fox-Wolfram moment [19], computed using all charged particles and EMC clusters not matched to tracks, be less than 0.3.

C. Fisher Discriminant

To further reduce continuum background, we combine several event-shape variables into a Fisher discriminant [20] F. Discriminating power originates from the observation that $q\bar{q}$ events tend to be jet-like, whereas $B\bar{B}$ events have a more spherical energy distribution. Rather than applying requirements on F, we use the corresponding distribution in the fits described in Sec. III E

Our Fisher discriminant is a linear combination of variables chosen, according to Monte Carlo studies, to maximize the separation between $B\bar{B}$ and continuum events. The first nine variables describe the energy flow inside nine concentric cones centered around the direction of the reconstructed $D^{*\pm}$. In addition, we use the momenta of the charged and the neutral particle closest to the cone axis, the polar angles in the CM of the reconstructed D^* momentum and the thrust axis T for charged tracks in the B_{tag} vertex (see next paragraph), the angle between the reconstructed D^* momentum and T, and the sum $S = \Sigma_i p_i \times P_2(\cos\theta_i)$ over the B_{tag} charged tracks, in which p_i is momentum, P_2 is the 2nd Legendre polynomial of argument $\cos\theta_i$, and θ_i is the angle between track i at the origin and T.

D. Flavor Tagging and Decay Time Measurement

For this analysis, two measurements are needed: the difference Δt between the proper decay times of the partially reconstructed B meson and the other B meson in the event, and the flavor of the latter.

The flavor tagging algorithm is based on tracks identified as leptons or kaons. These must be chosen among those not used in B_{rec} reconstruction and must originate from within 4 mm (3 cm) of the interaction point in the transverse (longitudinal) view.

The momentum of the lepton candidates is required to be greater than 1.1 GeV/c in order to reject most leptons from charmed meson decays. If one or more lepton candidates are qualified, the tag flavor is assigned based on the charge of the lepton with the highest center-of-mass momentum. If two or more qualified kaons are present, the event is used only if the flavor is unambiguous. If both a lepton and a kaon tag are available, the lepton tag is used.

The time difference Δt is calculated using $\Delta t = \Delta z/\gamma\beta c$, where $\Delta z = z_{rec} - z_{tag}$ is the difference between the z-coordinates of the partially reconstructed B_{rec} and B_{tag} vertices and the boost parameters are calculated using the measured beam energies. The uncertainty $\sigma_{\Delta t}$ on Δt is calculated from the results of the z_{rec} and z_{tag} vertex fits. We require $|\Delta t| < 20\,\text{ps}$ and $\sigma_{\Delta t} < 2.5\,\text{ps}$.

We define the B_{rec} vertex as the decay point of the fully reconstructed $D^{*\pm}$. The π_s track from the other $D^{*\pm}$ is not used, since it undergoes significant multiple Coulomb scattering and hence does not improve the z_{rec} measurement resolution.

The B_{tag} vertex reconstruction depends on the tagging category. For kaon-tagged events, we obtain z_{tag} from a beam spot constrained vertex fit of all charged tracks in the event, excluding those from the B_{rec} meson, and excluding also tracks within 1 rad of the unreconstructed D^0 momentum in the CM frame, which presumably originate from the D^0 decay. We require the probability of this fit to be greater than 10^{-2}. For lepton-tagged events, we use the lepton track parameters and errors, and the measured beam spot position and size in the plane perpendicular to the beams (the x-y plane). We find the position of the point in space for which the sum of the χ^2 contributions from the lepton track and the beam spot is minimum. The z coordinate of this point is taken as z_{tag}.

The beam spot is measured on a run-by-run basis using 2-prong events (Bhabha and $\mu^+\mu^-$), and has an r.m.s. size of approximately 120 μm in the horizontal dimension (x), 5 μm in the vertical dimension (y), and 8.5 mm along the beam direction (z). The average B meson flight distance in the x-y plane is 30 μm. To account for the B flight distance in the beam spot constrained vertex fit, 30 μm are added in quadrature to the effective x and y sizes.

E. Probability Distribution Functions

We use two PDF's, P_{on} for on-resonance, and P_{off} for off-resonance data. The former depends on the variables m_{rec}, F, Δt, $\sigma_{\Delta t}$, S_{tag}, and is given by the sum of the PDF's for the different event types described above:

$$P_{on} = f_{B\bar{B}}\left[f_{sig}P_{sig} + (1 - f_{sig})P_{comb}\right] + (1 - f_{B\bar{B}})P_{q\bar{q}} \quad (4)$$

where P_{sig}, P_{comb}, and $P_{q\bar{q}}$ are respectively the PDF's for signal events, for combinatorial background from $B\bar{B}$, and for continuum. Moreover, $f_{B\bar{B}}$ is the fraction of $B\bar{B}$

events in our sample, and f_{sig} is the fraction of signal events in $B\bar{B}$ events. The PDF for off-resonance data, P_{off}, is reduced to just one component, $P_{q\bar{q}}$, as the off-peak sample contains only continuum events.

According to Monte Carlo, the distributions of $B^0\bar{B}^0$ and B^+B^- combinatorial background events are very similar and can be described well by the same PDF.

We do not consider the fraction of $B\bar{B}$ events a free parameter, but fix it to $f_{B\bar{B}} = 1 - f_{q\bar{q}}$, where $f_{q\bar{q}}$ is the fraction of continuum events in the on-peak sample and is defined by

$$f_{q\bar{q}} = \frac{N_{\text{off-peak}}}{N_{\text{on-peak}}} \frac{\mathcal{L}_{\text{on-peak}}}{\mathcal{L}_{\text{off-peak}}}, \tag{5}$$

where N's are the number of events left by our selection in the on- and off-peak samples and $\mathcal{L}$'s are the integrated on- and off-peak luminosities.

Each of the P_i ($i = \text{sig, comb}, q\bar{q}$) can be expressed as the product of three one dimensional PDF's:

$$P_i(m_{\text{rec}}, F, \Delta t, \sigma_{\Delta t}, S_{\text{tag}}) = \tag{6}$$
$$\mathcal{M}_i(m_{\text{rec}}) \, \mathcal{F}_i(F) \, T'_i(\Delta t, \sigma_{\Delta t}, S_{\text{tag}}),$$

that are the probability distributions of the recoil D^0 mass $\mathcal{M}_i(m_{\text{rec}})$, the Fisher discriminant function $\mathcal{F}_i(F)$, and the decay time difference function $T'_i(\Delta t, \sigma_{\Delta t}, S_{\text{tag}})$. This follows from extensive Monte Carlo studies showing that the correlations among these variables are negligible.

1. $\mathcal{M}(m_{\text{rec}})$ and $\mathcal{F}(F)$ PDF's

The m_{rec} distribution of all sample components can be well modelled in the lower region of the spectrum with a so called "Argus function" [21]:

$$\mathcal{A}(m_{\text{rec}}) = m_{\text{rec}}\sqrt{1 - (m_{\text{rec}}/m_{\text{ep}})^2} \cdot e^{c \cdot m_{\text{rec}}/m_{\text{ep}}}, \tag{7}$$

where m_{ep} is the kinematic endpoint ($m_{\text{rec}} \leq m_{\text{ep}}$) and c is a free parameter describing the slope. This function alone, however, is not sufficient to account for the abrupt fall of the m_{rec} spectrum near the kinematic endpoint. For the signal sample we model this shoulder with an asymmetric error function with widths σ_l and σ_r, tapered off at low m_{rec} by an exponential factor with decay constant a:

$$\mathcal{E}(m_{\text{rec}}) =$$
$$\begin{cases} e^{m_{\text{rec}}/a}[1 - \text{erf}(m_{\text{rec}} - m_{\text{ep}})/(\sqrt{2}\sigma_l)], & m_{\text{rec}} < m_{\text{ep}} \\ e^{m_{\text{rec}}/a}[1 - \text{erf}(m_{\text{rec}} - m_{\text{ep}})/(\sqrt{2}\sigma_r)], & m_{\text{rec}} > m_{\text{ep}}. \end{cases}$$

Thus, we describe the signal m_{rec} distribution with a combination of three functions: a Gaussian G having average m_G and standard deviation σ_G for the well reconstructed peaking component; an Argus function, mainly for events in which the right D^* is combined with a low-momentum pion from another decay chain; and the $\mathcal{E}$

function:

$$\mathcal{M}_{\text{sig}}(m_{\text{rec}}) = f_{\text{sig}}^{\mathcal{A}} \cdot \mathcal{A}(m_{\text{rec}}) +$$
$$+ (1 - f_{\text{sig}}^{\mathcal{A}}) \cdot \Big[f^G \cdot G(m_{\text{rec}}) \qquad (8)$$
$$+ (1 - f^G) \cdot \mathcal{E}(m_{\text{rec}}) \Big].$$

In Eq. 8 $f_{\text{sig}}^{\mathcal{A}}$ is the fraction of events described by the Argus component and f^G is the fraction of events in the Gaussian peak relative to the non-Argus component.

For the background, both combinatorial and continuum, we set the fraction of the Gaussian component to zero, and model the distribution at the endpoint with a simple error function of width σ. However, for the case of combinatorial background in kaon-tagged events, we find that two different Argus components ($\mathcal{A}_1$ and $\mathcal{A}_2$) are needed to correctly describe the entire reconstructed mass spectrum. We thus define two PDF's according to:

$$\mathcal{M}_{\text{comb}}(m_{\text{rec}}) = f_{\text{comb}}^{\text{erf}} \cdot \text{erf}(m_{\text{rec}} - m_{\text{ep}}; \sigma_{\text{comb}}) +$$
$$+ (1 - f_{\text{comb}}^{\text{erf}}) \cdot \Big[f_{\text{comb}}^{\mathcal{A}_1} \cdot \mathcal{A}_1(m_{\text{rec}}) +$$
$$+ (1 - f_{\text{comb}}^{\mathcal{A}_1}) \cdot \mathcal{A}_2(m_{\text{rec}}) \Big], \tag{9}$$

$$\mathcal{M}_{q\bar{q}}(m_{\text{rec}}) = f_{q\bar{q}}^{\text{erf}} \cdot \text{erf}(m_{\text{rec}} - m_{\text{ep}}); \sigma_{q\bar{q}} +$$
$$+ (1 - f_{q\bar{q}}^{\text{erf}}) \cdot \mathcal{A}_1(m_{\text{rec}}). \tag{10}$$

The parameter m_{ep} represents simultaneously the two Argus endpoints and the error function inflection point.

The Fisher discriminant PDF $\mathcal{F}_i$ is parameterized by two Gaussian functions for each event type $i = (B\bar{B}, q\bar{q})$, having standard deviations σ_i^L and σ_i^R, and common mean μ_i:

$$\mathcal{F}_i(F) \propto \begin{cases} \exp\left[-(F - \mu_i)^2/2(\sigma_i^L)^2\right] & F < \mu_i \\ \exp\left[-(F - \mu_i)^2/2(\sigma_i^R)^2\right] & F > \mu_i. \end{cases} \tag{11}$$

Since the Fisher variable is designed to discriminate between $q\bar{q}$ and $B\bar{B}$ events, we expect the Fisher discriminant for signal events to be indistinguishable from that of $B\bar{B}$ combinatorial events. We have verified this expectation with Monte Carlo studies, and thus use the same Fisher discriminant to describe both event types.

2. Δt PDF's

The Δt-dependent part of the PDF is a convolution of the form

$$T'_i(\Delta t, \sigma_{\Delta t}, S_{\text{tag}}) =$$
$$\int d\Delta t_{\text{true}} \, T_i(\Delta t_{\text{true}}, S_{\text{tag}}) \, \mathcal{R}_i(\Delta t - \Delta t_{\text{true}}, \sigma_{\Delta t}), \tag{12}$$

where T is the distribution of Δt_{true}, the true decay time difference, and $\mathcal{R}$ is a resolution function that parameterizes detector resolution and systematic offsets in the measured positions of vertices.

Taking into account the mistag probability and the effect of tags due to the unreconstructed D^0, the Δt signal PDF in Eq. 12 can be written as

$$
\begin{aligned}
T_{\text{sig}} =\ & \tfrac{1}{4\tau_b}\, e^{-|\Delta t_{\text{true}}|/\tau_b} \cdot \Big\{ 1 - S_{\text{tag}}\,\Delta\omega(1-\alpha)+ \\
& + S_{\text{tag}}\,(1-2\omega)\,(1-\alpha) \\
& \cdot [C\cos(\Delta m_d \Delta t_{\text{true}}) + S\,\sin(\Delta m_d \Delta t_{\text{true}})] \Big\},
\end{aligned} \tag{13}
$$

where α (see Sec. IV B) is the fraction of events in which the tagging track is from the unreconstructed D^0, $\omega \equiv (\omega^+ + \omega^-)/2$ is the average mistag rate, and $\Delta\omega \equiv \omega^+ - \omega^-$ is the mistag rate difference between B^0 and $\bar{B}^0$ tags. The time-dependent CP asymmetry parameters S and C are the object of the measurement discussed in the present article.

Since the $B\bar{B}$ combinatorial background is dominated by non-CP final states, the CP asymmetry is expected to be negligible. However, we allow the PDF to accommodate some contamination from CP final states. Therefore, we parameterize the $B\bar{B}$ background Δt distribution with a PDF similar to that for signal events given in Eq. 13. We also add a fraction f_δ of a δ-function, to allow for a zero-lifetime component:

$$
\begin{aligned}
T_{\text{comb}} =\ & f^\delta_{\text{comb}} \cdot \delta(|\Delta t_{\text{true}}|)\left(1 - S_{\text{tag}}\,\Delta\omega^\delta_{\text{comb}}\right)+ \\
& +(1-f^\delta_{\text{comb}}) \cdot \tfrac{1}{4\tau_{\text{comb}}}\, e^{-|\Delta t_{\text{true}}|/\tau_{\text{comb}}} \\
& \cdot \Big\{ 1 - S_{\text{tag}}\,\Delta\omega_{\text{comb}}+ \\
& + S_{\text{tag}} \cdot \big[C_{\text{comb}}\cos(\Delta m_d \Delta t_{\text{true}})+ \\
& + S_{\text{comb}}\,\sin(\Delta m_d \Delta t_{\text{true}}) \big] \Big\}.
\end{aligned} \tag{14}
$$

The second term of the PDF is obtained from Eq. 13 with $\omega = \alpha = 0$, as these are not defined for background events. The $C_{\text{comb}}, S_{\text{comb}}$ parameters describe small fluctuations in the Δt distribution of background events and possible CP event contamination, leading to a small effective CP violation value.

The $\Delta\omega$ parameters, which for signal events is the difference in the mistag probabilities for B^0 and $\bar{B}^0$, allow for differences in the number of events tagged as a B^0 or $\bar{B}^0$ in the same background sample. We use this PDF to describe both the $B^0\bar{B}^0$ and B^+B^- components.

The PDF for the background due to continuum events is modeled with a simple exponential decay distribution plus a fraction f_δ of a δ-function:

$$
\begin{aligned}
T_{q\bar{q}} =\ & f^\delta_{q\bar{q}} \cdot \left(1 - S_{\text{tag}}\,\Delta\omega^\delta_{q\bar{q}}\right) \cdot \delta(|\Delta t_{\text{true}}|)+ \\
& + (1-f^\delta_{q\bar{q}}) \cdot \left(1 - S_{\text{tag}}\Delta\omega_{q\bar{q}}\right) \cdot \tfrac{1}{4\tau_{q\bar{q}}}\, e^{-|\Delta t_{\text{true}}|/\tau_{q\bar{q}}}
\end{aligned} \tag{15}
$$

where the parameters $\Delta\omega^\delta_{q\bar{q}}$ and $\Delta\omega_{q\bar{q}}$ allow for differences in the number of events tagged as a B^0 or $\bar{B}^0$ in this sample.

3. Resolution Functions

The resolution function for events of type i (i=sig, comb, $q\bar{q}$) is parameterized as the sum of three Gaussian functions:

$$
\begin{aligned}
\mathcal{R}_i(t_r, \sigma_{\Delta t}) =\ & f^n_i\,\mathcal{G}^n_i(t_r, \sigma_{\Delta t}) \\
& + (1 - f^n_i - f^o_i)\,\mathcal{G}^w_i(t_r, \sigma_{\Delta t}) \\
& + f^o_i\,\mathcal{G}^o_i(t_r),
\end{aligned} \tag{16}
$$

where $t_r = \Delta t - \Delta t_{\text{true}}$ is the residual of the Δt measurement, and $\mathcal{G}^n_i$, $\mathcal{G}^w_i$, and $\mathcal{G}^o_i$ are the "narrow", "wide", and "outlier" Gaussian functions. The narrow and wide Gaussian functions incorporate information from the Δt uncertainty $\sigma_{\Delta t}$, and account for systematic offsets in the estimation of $\sigma_{\Delta t}$ and the Δt measurement. They have the form

$$
\begin{aligned}
\mathcal{G}^k_i(t_r, \sigma_{\Delta t}) \equiv\ & \frac{1}{\sqrt{2\pi}\, s^k_i\, \sigma_{\Delta t}} \\
& \cdot \exp\left(-\frac{\left(t_r - b^k_i \sigma_{\Delta t}\right)^2}{2(s^k_i\, \sigma_{\Delta t})^2} \right),
\end{aligned} \tag{17}
$$

where the index k takes the values $k = n, w$ for the narrow and wide Gaussian funcions, and b^k_i and s^k_i are parameters determined by fits. The outlier Gaussian function, describing a small fraction of events with badly measured Δt, has the form

$$
\mathcal{G}^o_i(t_r) \equiv \frac{1}{\sqrt{2\pi}\, s^o_i} \exp\left(-\frac{(t_r - b^o_i)^2}{2(s^o_i)^2} \right). \tag{18}
$$

In all fits, the values of b^o_i and s^o_i are fixed to 0 ps and 8 ps, respectively, and are later varied to evaluate systematic uncertainties.

F. Analysis Procedure

After the event selection described in Sec. III B is complete, the rest of the analysis proceeds with a series of unbinned maximum-likelihood fits, performed simultaneously on the on- and off-resonance data samples and independently for the lepton-tagged and kaon-tagged events. The procedure can be logically divided in the following three steps, which we shall discuss in detail in the following paragraphs:

1. In the first step we determine the signal fraction f_{sig} in Eq. 4 and the shape of $\mathcal{M}(m_{\text{rec}})$ and $\mathcal{F}(F)$ in Eq. 6 for the different classes of events (signal and backgrounds, kaon and lepton tagging categories). This is done by fitting data with the PDF

$$
P_i(m_{\text{rec}}, F) = \mathcal{M}_i(m_{\text{rec}})\,\mathcal{F}_i(F), \tag{19}
$$

   ignoring the time dependence; we refer to this step as the kinematic fit.

2. In the second step we determine the tagging dilution due to wrong tag assignments.

3. In the last step we perform the time-dependent fit to the data. We fix all parameter values obtained in the previous steps and use the full PDF of Eq. 6 to determine the parameters of the resolution functions, $T_i'(\Delta t, \sigma_{\Delta t}, S_{\text{tag}})$, and the CP asymmetry values C, S of the signal and of the $B\overline{B}$ combinatorial background component.

The fitting procedure has been validated using both full Monte Carlo and, where the requested number of events would be too large, the technique of "toy" Monte Carlo. In a toy Monte Carlo, events are described by a small number of variables which are generated according to our PDF's.

IV. RESULTS

Event selection yields the numbers of events listed in the top two rows of Table I. The third and fourth rows

TABLE I: Event selection yield. The first uncertainty shown is statistical, while the second uncertainty on the number of continuum events accounts for a 1% relative uncertainty on the on-peak and off-peak luminosities.

	# of events	
	kaon tag	lepton tag
on-peak	61179	20855
off-peak	1025	51
continuum	$9814 \pm 307 \pm 196$	$488 \pm 68 \pm 10$
$B\overline{B}$	51365 ± 364	20367 ± 69
N_{sig}	3843 ± 397	1129 ± 218

show the number of continuum and $B\overline{B}$ events calculated, using Eq. 5, from the number of off-peak events in the second row. The numbers of signal events in the last line of the table are calculated using the signal fractions obtained from the kinematic fit described in the next section.

A. Kinematic Fit

We begin by fitting the shape of our signal, $\mathcal{M}_{\text{sig}}(m_{\text{rec}})$, using a large sample of Monte Carlo signal events. The parameters most relevant to determine directly the signal fraction in the data, and consequently our final result for S and C, will be released again in the final kinematic fit. They are (refer to Eq. 8): the Gaussian fraction f_G, mean value m_G, and standard deviation σ_G, and are shown in the last section of Table II.

Next we fit the Fisher $\mathcal{F}_{q\bar{q}}$ and recoil mass $\mathcal{M}_{q\bar{q}}$ distribution to the off-peak data sample. As the number of off-resonance events selected in the lepton tagged sample is too small to yield convergence, we set the lepton tag sample parameters to the corresponding values obtained from the fit to the kaon tag sample. Due to the small continuum fraction in the lepton sample, we judge that this does not introduce any significant systematic effect. The $\mathcal{F}_{q\bar{q}}$ parameters are fixed in all subsequent fits.

We initialize the parameters of the $B\overline{B}$ combinatorial background PDF directly from the data, using a sample of events in which the contribution of signal events is much reduced. We obtain this sample by combining a D^* with a pion of wrong sign charge (WS sample). We have verified, both on Monte Carlo and in the m_{rec} sideband for data, (1.836–1.856 GeV/c^2), that the shape of the $\mathcal{M}(m_{\text{rec}})$ distribution for combinatorial $B\overline{B}$ background is well described by that of the WS data sample.

To evaluate a possible contribution from a peaking component in the $B\overline{B}$ background events, we have allowed the Gaussian fraction f_G in Eq. 8 to float in a fit to a sample of Monte Carlo background events; this fraction is found to be 0.000 ± 0.002, and is therefore set to zero.

Finally we fit the on-peak data sample, leaving as free parameters the fraction f_{sig} of signal events in the $B\overline{B}$ component, some of the shape parameters of the continuum and $B\overline{B}$ combinatorial background $\mathcal{M}_{\text{comb}}$, some of the signal parameters in $\mathcal{M}_{\text{sig}}$, and the shape parameters of the Fisher discriminant $\mathcal{F}_{B\overline{B}}$. Table II summarizes the results and provides information about which parameters are released in the fit (statistical uncertainties given) and which ones are taken from previous fits (no uncertainty given).

The final results of the kinematic fits for the kaon and lepton tagged sample are shown in Fig. 3 and Fig. 4.

B. Determination of mistag probabilities

A common problem of analyses using the partial reconstruction technique is that a fraction of the tracks used in tagging may belong to the unreconstructed D^0, leading to a mistag of the event. As the tracks originating from the missing D^0 tend to align to its direction of flight, this fraction can be reduced by applying a constraint on the cosine of the CM opening angle θ_{tag} between the tagging track and the direction of the unreconstructed D^0. We require $\cos\theta_{\text{tag}} \leq 0.75$ (0.50) for the kaon (lepton) tagged sample.

We find from signal Monte Carlo that before this requirement 26% (13%) of kaon (lepton) tags originate from a missing D^0. We call these events "D-tags", while "T-tags" are those in which the tagging track (either direct or cascade) is from the tag B.

To reduce dependency on Monte Carlo the fraction α of D-tags remaining after the $\cos\theta_{\text{tag}}$ constraint is measured using data, as explained below.

TABLE II: Results of the final kinematic fits. The values of fixed parameters are given without uncertainties.

| PDF	parameter	description	kaon tags	lepton tags
	$f_{\rm sig}$	Signal fraction	$(7.5 \pm 0.7)\%$	$(5.5 \pm 1.1)\%$
$\mathcal{F}_{B\bar{B}}(F)$	$\mu_{B\bar{B}}$		0.723 ± 0.005	0.721 ± 0.009
	$\sigma^L_{B\bar{B}}$		0.361 ± 0.003	0.380 ± 0.006
	$\sigma^R_{B\bar{B}}$		0.469 ± 0.004	0.532 ± 0.006
	f^A	Argus fraction	1.0	1.0
	$m_{\rm ep}$	Argus endpoint (GeV/c^2)	1.8696	1.8696
$\mathcal{M}_{q\bar{q}}(m_{\rm rec})$	c	Argus exponent	-17 ± 9	-17
	$f_{\rm comb}$	erf fraction	0.52 ± 0.15	0.52
	$\sigma_{\rm comb}$	erf width (GeV/c^2)	0.0005 ± 0.0002	0.0005
	$f^{\mathcal{A}_1}$	Argus fraction	0.27 ± 0.06	1.0
	$m_{\rm ep}$	Argus end point (GeV/c^2)	1.8696	1.8695
$\mathcal{M}_{\rm comb}(m_{\rm rec})$	c_1	$\mathcal{A}_1$ exponent	-49 ± 38	-15 ± 2
	c_2	$\mathcal{A}_2$ exponent	-0.56 ± 0.25	$-$
	$f_{q\bar{q}}$	erf fraction	0.26 ± 0.04	0.41 ± 0.06
	$\sigma_{q\bar{q}}$	erf width (GeV/c^2)	$(75 \pm 9) \cdot 10^{-5}$	$(72 \pm 2) \cdot 10^{-5}$
	f_G	Gaussian fraction	0.46 ± 0.06	0.64 ± 0.12
$\mathcal{M}_{\rm sig}(m_{\rm rec})$	m_G	Gaussian peak (GeV/c^2)	1.8638 ± 0.0002	1.8635 ± 0.0003
	σ_G	Gaussian width (GeV/c^2)	0.0017 ± 0.0002	0.0019 ± 0.0003
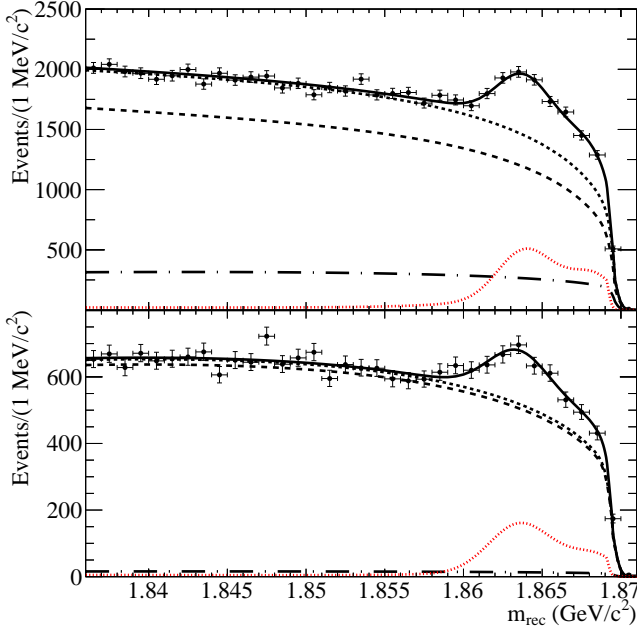
FIG. 3: Result of the kinematical fit of kaon (top) and lepton (bottom) tagged data events, with PDF's overlaid: total PDF (solid line), total background ($B\bar{B}$ + continuum, short-dashed line), $B\bar{B}$ combinatorial background (dashed line), continuum u,d,s,c background (dot-dashed line) and signal (dotted red line).
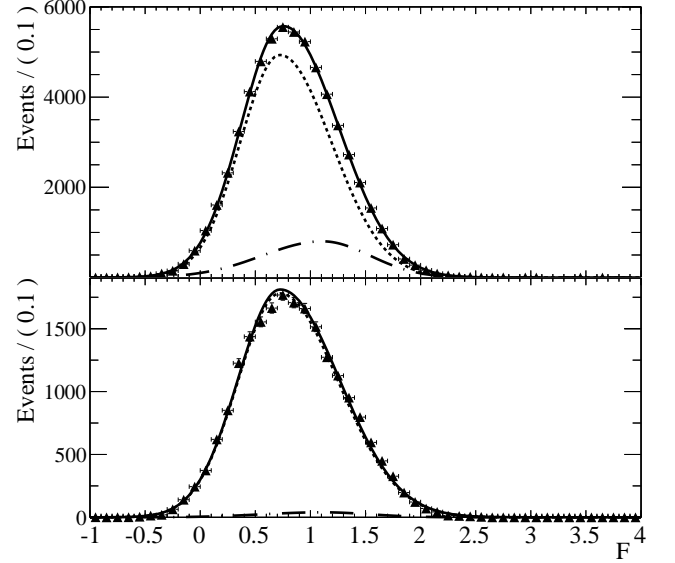

FIG. 4: Result of the kinematical fit of kaon (top) and lepton (bottom) tagged events for the Fisher function, with PDF's overlaid: total $B\bar{B}$ (solid line), $B\bar{B}$ (dashed line) and continuum u,d,s,c background (dash-dotted line).

Defining the total number N_T (N_D) of T (D) tags, the number N_T^l (N_D^l) of them that satisfy the $\cos\theta_{\rm tag}$ requirement, and the number N_T^g (N_D^g) of them that do not, α is given by:

$$\alpha = N_D^l/(N_D^l + N_T^l) = \frac{f^D p^D}{(f^D p^D + (1-f^D)p^T)}, \quad (20)$$

where $p^T = N_T^l/N_T$ ($p^D = N_D^l/N_D$) is the probability,

taken from signal Monte Carlo, for a T-tag (D-tag) to be from a track satisfying the $\cos\theta_{\text{tag}}$ cut. The fraction of D-tags, $f^D = N_D/(N_T + N_D)$, is given by

$$f^D = (p^T - f^l)/(p^T - p^D). \qquad (21)$$

The fraction $f^l = N^l/(N^l + N^g)$ is obtained from the kinematic fit of the data: N^l is the number of signal events that have $\cos\theta_{\text{tag}} \leq 0.75$ (0.50) and N^g is the number of signal events with $\cos\theta_{\text{tag}} \geq 0.75$ (0.50) for kaon (lepton) tag events.

In this way we obtain the values $\alpha = 0.12 \pm 0.04$ for kaon tags and $\alpha = 0.00 \pm 0.02$ for lepton tags, as shown in Table III, where we also list the mistag parameters ω and $\Delta\omega$, α, τ_b, and Δm_d that we will need in the final Δt fit.

We use information from signal Monte Carlo events to determine the mistag probability $\omega = 0.201 \pm 0.002$ (0.101 ± 0.002) and mistag difference $\Delta\omega = -0.011 \pm 0.003$ (0.001 ± 0.005) for the kaon (lepton) tagged samples. We use the world average value for Δm_d [18], and the values fitted to signal Monte Carlo for τ_b, as discussed in Sec. III B.

TABLE III: Values of mistag parameters and α used in the final fit. The b lifetime values were obtained from the fit of signal Monte Carlo. The statistical uncertainties are given.

parameter	kaon tags	lepton tags
ω	0.201 ± 0.002	0.104 ± 0.002
$\Delta\omega$	-0.011 ± 0.003	0.001 ± 0.005
α	0.12 ± 0.04	0.0 ± 0.02
τ_b (ps)	1.458 ± 0.014	1.518 ± 0.018
Δm_d (ps^{-1})	0.507 ± 0.004	

C. Time Dependent Fit

After the kinematic fit is complete and mistag probabilities are determined, we can proceed to the final Δt fit to extract the CP-violating parameters S and C.

We start by fitting the signal Δt PDF and its resolution function using a pure signal Monte Carlo sample; the parameters determined in this way will be used to initialize the signal PDF, and some of them will be left free again in the final Δt fit.

Next we fit the resolution function parameters and the effective lifetime of the continuum background, using the off-peak data sample. For the kaon tag sample, the data strongly disfavor a component with nonzero lifetime, therefore we fix $f_\delta = 1$, and leave free in the final Δt fit only $\Delta\omega_\delta$ from Eq. 15. For lepton tags, as the real data sample is too small, we obtain resolution and Δt parameters from continuum Monte Carlo.

We use the continuum parameters obtained above in the next fit stage, where we obtain the $B\bar{B}$ background resolution function and Δt parameters using real data, by restricting the fit to events in a sideband region (1.836–1.856 GeV/c^2) of the D^0 recoil mass distribution. According to Monte Carlo studies the fraction of signal events in this sideband is negligible, and we set it to zero. We fit simultaneously the resolution and lifetime parameters, shown in sections 1 and 3 of Table IV. The fitted values of C_{comb} and S_{comb} are consistent with 0 as expected.

We are now in a position to perform the final Δt fit, in which we release parameters from the signal, continuum and $B\bar{B}$ combinatorial background Δt and resolution models, as detailed in Table IV, always with the convention that parameters free (fixed) in the final Δt fit are shown with (without) a fit uncertainty.

The results are also shown in Fig. 5 (6) for the kaon (lepton) tagged samples, where we plot the Δt distributions separately for B^0 and $\bar{B}^0$ tags, together with the time-dependent raw CP asymmetry

$$A(\Delta t) = \frac{N_{S_{\text{tag}}=1}(\Delta t) - N_{S_{\text{tag}}=-1}(\Delta t)}{N_{S_{\text{tag}}=1}(\Delta t) + N_{S_{\text{tag}}=-1}(\Delta t)}. \qquad (22)$$

For presentation purposes, only data in the restricted signal region $m_{\text{rec}} > 1.860$ GeV/c^2 are shown in Fig. 5 and Fig. 6, in order to amplify signal/background ratio and be able to see the oscillation. The signal fractions in this region become $\approx 24\%$ and $\approx 18\%$ for kaon and lepton tags respectively.

This requirement is not applied to the fit sample, so our numeric results apply to the whole signal region $m_{\text{rec}} > 1.836$ GeV/c^2.

V. SYSTEMATIC UNCERTAINTIES

Our systematic uncertainties on the CP-violating parameters S and C are summarized in Table V. We discuss here the most significant ones.

Most systematic uncertainties in Table V are due to imperfect knowledge of one single parameter fixed in the final Δt fit, having little or no correlation with uncertainties of other parameters. They have been treated by varying them by $\pm 1\sigma$ and repeating the final Δt fit leaving only the parameters S and C free to vary.

Uncertainties in the first two lines have a different character because they are due to parameter sets, in which correlations among parameters belonging to one set are non-trivial. Given the low signal-to-background ratio, correct modelling of the background shape and signal fraction in the kinematic fit is crucial, especially because the $\mathcal{M}(m_{\text{rec}})$ and $\mathcal{F}(F)$ PDF's parameters are fixed in the final Δt fit. Consequently, we devised a procedure to evaluate the associated systematic uncertainties, that would also preserve the correlations among parameters belonging to a set.

TABLE IV: Result of the final full fit. The values of fixed parameters are given without uncertainties.

PDF	parameter	description	kaon tags	lepton tags
$B\bar{B}$ resolution model	b^n	offset of narrow Gaussian	-0.16 ± 0.01	-0.022 ± 0.014
	b^o	offset of outlier Gaussian (ps)	0.0	0.0
	b^w	offset of wide Gaussian	-1.0 ± 0.2	-0.7 ± 0.7
	f^n	fraction of narrow Gaussian	0.93 ± 0.01	0.977 ± 0.004
	f^o	fraction of outlier Gaussian	0.008 ± 0.001	0.006 ± 0.002
	s^n	see eq. 17	1.03 ± 0.03	1.02 ± 0.02
	s^o	see eq. 18 (ps)	8.0	8.0
	s^w	see eq. 17	3.0	5.6
continuum Δt	$\Delta\omega_{q\bar{q}}^{\delta}$	see eq. 15	-0.04 ± 0.02	0.03
$B\bar{B}$ Δt	$f_{\rm comb}^{\delta}$	see eq. 14	0.10 ± 0.02	0.25 ± 0.02
	$\Delta\omega_{\rm comb}^{\delta}$	see eq. 14	0.04 ± 0.12	-0.08 ± 0.07
	$\Delta\omega_{\rm comb}$	see eq. 14	-0.025 ± 0.012	0.012 ± 0.021
	$\tau_{\rm comb}$	effective lifetime (ps)	1.318 ± 0.023	1.272 ± 0.031
	$C_{\rm comb}$	cosine coefficient	-0.022 ± 0.024	-0.024 ± 0.041
	$S_{\rm comb}$	sine coefficient	0.004 ± 0.014	-0.023 ± 0.024
signal resolution model	b^n	offset of narrow Gaussian	-0.35 ± 0.09	-0.3 ± 0.2
	b^w	offset of wide Gaussian	8 ± 3	$-$
	f^n	fraction of narrow Gaussian	0.992 ± 0.007	1.0 ± 0.1
	f^o	fraction of outlier Gaussian	0.0	$-$
	s^n	see eq. 17	1.13 ± 0.12	1.17 ± 0.21
	s^w	see eq. 17	2.6	$-$
signal Δt	C		$+0.117 \pm 0.111$	$+0.195 \pm 0.147$
	S		-0.417 ± 0.159	-0.210 ± 0.200

For each set of parameters in $\mathcal{M}$ or $\mathcal{F}$ that become fixed at any stage of our fits, and are not released again in the final Δt fit, a large number N_t of toy Monte Carlo experiments of the same size as the data are generated and fitted, and the values of parameters in the N_t experiments are saved. Evaluation of the systematics due to a set of parameters in subsequent fits (in which they become fixed) is made by repeating the latter fits many times over, using the same event sample, but fixing parameters in the set to different values every time, taken from one of the N_t experiments. In this way, we propagate the variation associated to parameter sets from one fit to the next one, and preserve correct correlations among them. We applied this procedure to obtain the uncertainties in lines 1 and 2 of Table V, which for lepton tagged events are the main source of systematics.

For lepton tags we find that only one Gaussian is sufficient to describe the resolution function ($f^n = 1$). The systematic due to the signal s^w was evaluated only for kaon tagged events.

Since the mistag parameter ω is obtained from Monte Carlo with a very small statistical uncertainty (see Table III), we verified the agreement between Monte Carlo and data using a control sample of self-tagging $B^0 \rightarrow D^{*\mp}\pi^{\pm}$ events. As a result of this study, we assign a very conservative uncertainty of 15% on ω, and evaluate the associated systematic by repeating the final Δt fit

varying its central value by $\pm 15\%$. This is the largest systematic uncertainty for kaon tagged events.

We estimate the systematic uncertainty associated with fixing the peaking background fraction f_G in Eq. 8 to zero by setting it to ± 0.002 for both the kaon and lepton tag samples, repeating the fit, and taking the largest deviation from the value fitted with $f_G = 0$ as the systematic uncertainty.

The signal $m_{\rm rec}$ spectra for the CP-even and CP-odd components are different, the latter being slightly harder. This may cause a small acceptance difference of our event reconstruction and selection, leading to a systematic shift in the C and S measurement. We have carefully evaluated this effect and found it to be negligible.

As the $D^{*+}D^{*-}$ final state is a superposition of CP-even and CP-odd wave functions, the measured values S and C from our data only represent a weighted average of these components, with their inverse squared errors as weights. Since the background shape is not uniform as it goes to zero at the kinematical limit, the weight of the CP-odd component could be enhanced with respect to the CP-even one by the lower background level in the high mass region. To evaluate this effect, we perform Δt fits in the two extreme Monte Carlo configurations, adding to the background sample a pure CP-odd ($R_\perp = 1$) or CP-even ($R_\perp = 0$) sample of signal events, respectively. The number of signal events in both cases

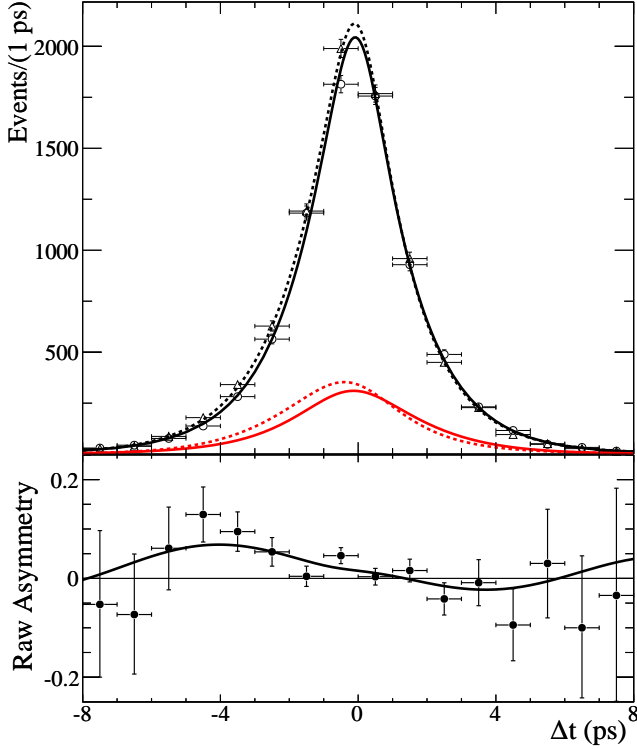FIG. 5: Top: Δt distribution for B^0 (dashed) and $\overline{B}^0$ (solid) kaon tags; the lower curves are the corresponding signal PDFs. Bottom: raw time-dependent CP asymmetry. Only data in the restricted signal region $m_{rec} > 1.860$ GeV/c^2 are shown.
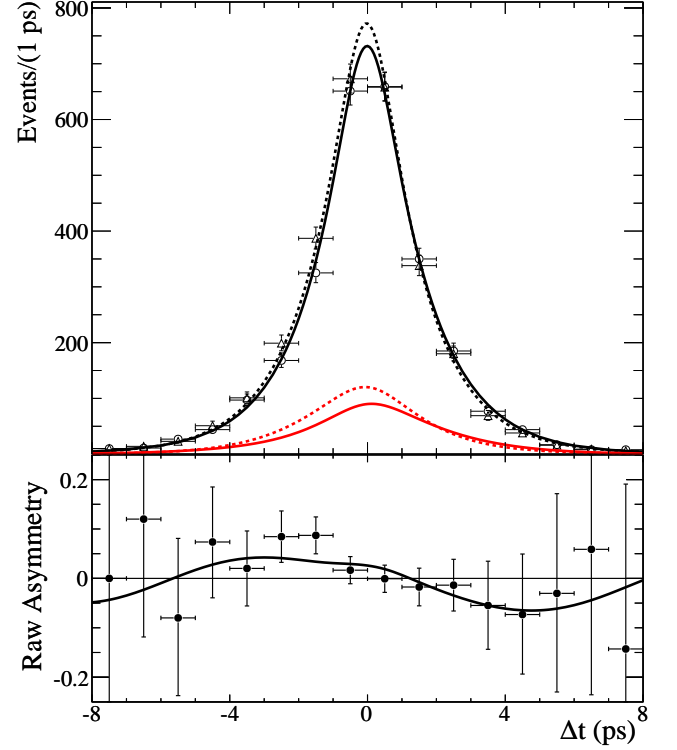
FIG. 6: Top: Δt distribution for B^0 (dashed) and $\overline{B}^0$ (solid) lepton tags; the lower curves are the corresponding signal PDFs. Bottom: raw time-dependent CP asymmetry. Only data in the restricted signal region $m_{rec} > 1.860$ GeV/c^2 are shown.

is equal to the number of signal events found in data. We find that the differences in the errors of S and C are negligible in these two cases and we do not assign a systematic uncertainty to this effect.

As discussed in Sec. IV C, τ_b and Δm_d are fixed to the values listed in Table III. We assign the systematic uncertainty due to these assumptions by varying their nominal values of $\pm 1\sigma$, and taking half the difference in the fitted values of C and S so obtained.

To evaluate bias on C and S in our fit, we apply the fit procedure to pure signal Monte Carlo events and compare the results for C and S to the generated ones; no significant bias has been observed in either. We therefore quote the statistical uncertainty on these Monte Carlo measurements as the associated systematic uncertainties.

To measure the systematic uncertainty related to imperfect knowledge of the time measurement due to uncertainty in the boost or possible uncorrected misalignment of the SVT, we repeat the time-dependent fit with different sets of realistic misalignments of the SVT and Δt scaling factors. The maximum observed shift with respect to the nominal fit is quoted as the uncertainty.

An important source of systematic uncertainty in our analysis is represented by interference effects from doubly Cabibbo-suppressed decay amplitudes on the tagging side of the event. The non-leptonic B-meson decays used for tagging are dominated by amplitudes containing a $b \to c\bar{u}d$ transition, thus ensuring the correlation of the tagging particle (typically a kaon) with the flavor of the originating b quark. However, $\bar{b} \to \bar{u}c\bar{d}$ transitions could also contribute, although they are suppressed[22] by a factor $r' \simeq |(V_{ub}^* V_{cd})/(V_{cb} V_{ud}^*)| = 0.02$.

As discussed in detail in Ref. [22], this effect cannot be simply reabsorbed into the mistag probability ω because the allowed and doubly Cabibbo-suppressed amplitudes can interfere, and thus effectively change the Δt probability density function.

Since our Δt PDF assumes $r' = 0$ and therefore does not include these effects, the C, S parameters measured by our fit will be different from the observables without tag-side interference by a calculable quantity.

To evaluate the systematic effect in our measurement due to neglecting small terms in the PDF with $r' \neq 0$, we follow the prescription in Ref. [22] and perform a simple toy Monte Carlo of $\delta C \equiv C_{fit} - C_0$ and $\delta S \equiv S_{fit} - S_0$, finding the results reported in Table V. The lepton tags are not affected by this issue.

TABLE V: Systematic uncertainties evaluated for C and S. Uncertainties in the top section are independent for kaon and lepton tags, those in the bottom section are correlated.

Systematic source	kaon tags		lepton tags	
	C	S	C	S
Kinematic fit parameters	0.013	0.034	0.023	0.057
Continuum Δt fit parameters	0.002	0.001	–	–
Signal s_w	0.0002	0.0007	–	–
$B\bar{B}$ combinatorial s_w	0.017	0.0007	0.001	0.005
Signal tag side (ω)	0.012	0.045	0.002	0.002
Mistag difference ($\Delta\omega$)	0.007	0.0004	0.007	0.0009
Signal CP side (α_{D^0})	0.006	0.017	0.002	0.002
Peaking background	0.0002	0.0003	0.0002	0.00004
Fit bias (MC statistics)	0.011	0.018	0.012	0.019
Tag interference from DCSD	0.030	0.002	–	–
B^0 lifetime variation	0.0002	0.002	0.0003	0.004
Δm_d variation	0.0003	0.001	0.0004	0.002
SVT misalignment	0.003	0.007	0.002	0.004
Boost uncertainty	0.002	0.006	0.005	0.007
Total	0.042	0.062	0.028	0.061

VI. PHYSICS RESULTS

The final results for C and S, with their correlation coefficient ρ, including only the statistical uncertainty for kaon and lepton tags, are:

$$\begin{aligned} C &= +0.12 \pm 0.11 \\ S &= -0.42 \pm 0.16 \end{aligned} \quad \rho = 0.0601, \quad \text{kaon tags,}$$

$$\begin{aligned} C &= +0.20 \pm 0.15 \\ S &= -0.21 \pm 0.20 \end{aligned} \quad \rho = 0.0730, \quad \text{lepton tags.}$$

The two samples are statistically independent of each other and can therefore be combined; their statistical uncertainties can be combined in quadrature, but the systematic ones need a more careful treatment.

Indeed, several of the systematic effects listed in Table V are independent for the kaons and lepton tags and are combined in quadrature, while the others are combined taking into account their correlation. Finally we get the combined results of this analysis of

$$\begin{aligned} C &= +0.15 \pm 0.09 \pm 0.04 \\ S &= -0.34 \pm 0.12 \pm 0.05 \end{aligned} \quad \rho = 0.0649.$$

A. Extraction of S_+ and C_+

The measured values of S and C that we obtain from data only represent a weighted average of the CP even and CP odd wave function components. If penguin amplitudes can be neglected then $S_+ = -S_-$, $C_+ = -C_-$ and the value of the CP-even components S_+ and C_+,

which we are interested in, can be obtained using the relations:

$$\begin{aligned} C &= C_+ \\ S &= S_+ \left(1 - 2R_\perp\right), \end{aligned}$$

where the factor $(1 - 2R_\perp)$ represents the dilution introduced by the CP-odd component $R_\perp$ in the signal. To compute S_+ we use the value measured by BABAR of $(R_\perp = 0.158 \pm 0.029)$ [8], where the uncertainty is the combined statistical and systematic. To evaluate the related systematic uncertainty, we vary this value by $\pm 1\sigma$. We obtain

$$\begin{aligned} C_+ &= +0.15 \pm 0.09 \pm 0.04 \\ S_+ &= -0.49 \pm 0.18 \pm 0.07 \pm 0.04, \end{aligned}$$

where the uncertainties shown are statistical and systematic; the third uncertainty is the contribution from the error on $R_\perp$ described above.

VII. SUMMARY

We have measured the time-dependent CP asymmetry parameters C and S in $B^0 \to D^{*+}D^{*-}$ decays, from which we have extracted the CP-even components S_+ and C_+. This result is an independent determination of the CP-violating parameters of $b \to (c\bar{c})d$ transitions and is compatible with previous measurements from BABAR [8] and Belle [9] using fully reconstructed decays. It also agrees well with the Standard Model expectation of negligible contributions to the decay amplitude from penguin diagrams and thence with $S_+ = -\sin 2\beta$.

---

[1] N. Cabibbo, Phys. Rev. Lett. **10**, 531 (1963).

[2] M. Kobayashi and T. Maskawa, Prog. Theor. Phys. **49**, 652 (1973).

[3] B. Aubert et al. (*BABAR* collaboration), Phys. Rev.D **79**, 072009 (2009).

[4] K. F. Chen et al. (Belle collaboration), Phys. Rev. Lett. **98**, 031802 (2007).

[5] H. Sahoo for the Belle collaboration, e-Print:arXiv:1109.4780[hep-ex].

[6] Z. Z. Xing, Phys. Lett. B **443**, 365 (1998).

[7] Z. Xing, Phys. Rev. D **61**, 014010 (1999).

[8] B. Aubert et al. (*BABAR* collaboration), Phys. Rev. D **79**, 032002 (2009).

[9] B. Vervink et al. (Belle collaboration), Phys. Rev. D **80**, 111104 (2009).

[10] Y. Grossman and M. P. Worah, Phys. Lett. B **395**, 241 (1997).

[11] M. Gronau, J. L. Rosner and D. Pirjol, Phys. Rev. D **78**, 033011 (2008).

[12] R. Zwicky, Phys. Rev. D **77**, 036004 (2008).

[13] B. Aubert et al. (*BABAR* collaboration), Nucl. Instrum. Meth. A **479**, 1 (2002).

[14] S. Agostinelli et al. (`GEANT4` collaboration), Nucl. Instrum. Meth. A **506**, 250 (2003).

[15] D. Lange and A. Ryd, `EvtGen`: a Monte Carlo Generator for *B*-Physics, Computing in High Energy Physics 1998, Chicago, Ill.(USA) (1998).

[16] W. Menges, IEEE Nuc. Sci. Symp. Conf. Rec. 2005, 3, 1470 (2006).

[17] Throughout this article, charge conjugate decay modes are implied.

[18] K. Nakamura et al. (Particle Data Group collaboration), J. Phys. G **37**, 075021 (2010).

[19] G. Fox and S. Wolfram, Phys. Rev. Lett. **41**, 1581 (1978).

[20] R. A. Fisher, Annals of Eugenics **7**, 179 (1936).

[21] H. Albrecht (ARGUS collaboration), Phys. Lett. B **340**, 217 (1994).

[22] O. Long, M. Baak, R. N. Cahn and D. Kirkby, Phys. Rev. D **68**, 034010 (2003).

[23] The Heavy Flavor Averaging Group, "Averages of *b*-hadron, *c*-hadron, and τ-lepton Properties", arXiv:1010.1589v1 [hep-ex].